JOURNAL OF PROPULSION AND POWER
Vol. 26, No. 1, January–February 2010

Near-Plume Laser-Induced Fluorescence Velocity Measurements of a Medium Power Hall Thruster

William A. Hargus Jr.* and Christopher S. Charles†
U.S. Air Force Research Laboratory, Edwards Air Force Base, California 93524

DOI: 10.2514/1.44411

This work presents the near exit plane velocity field of a 600 W Hall thruster at a single operating condition with a 300 V anode potential. The xenon ion propellant velocities were measured using laser-induced fluorescence of the $5d[4]_{7/2} - 6p[3]_{5/2}$ excited state xenon ionic transition at 834.72 nm. Ion velocities were interrogated from the acceleration channel exit plane to a distance 100 mm from the exit plane (1.6 exit plane diameters). Both axial and radial velocities were directly measured. A nearly uniform axial velocity profile of approximately 17,000 m/s (197 eV) was measured at the acceleration channel center on the exit plane. The maximum axial velocity was measured 100 mm from the exit plane at 19,800 m/s (267 eV). In conjunction with the coaxial symmetry of the thruster, radial velocity measurements were used to determine the divergence of the plume, as well as to determine azimuthal velocities in several regions proximate to the exit plane. The 475 m/s mean azimuthal velocity was measured 5 mm from the exit plane. From this value, it was possible to estimate a maximum thruster-induced torque of 3.2×10^{-5} Nm. Because of the divergence and convergence of the coaxial ion flow, distinct ion populations were observed to interact in the central core of the near plume. This was apparent in measurement volumes where multiple radial and axial velocity components were measured. These regions also typically correspond with the brightest portions of the visible plume.

I. Introduction

TO BETTER characterize the use of Hall thrusters for on-orbit propulsion applications, there is a need for improved understanding of the near exit plane xenon ion velocity field. Spacecraft interaction models have been developed which use near exit plane plasma information to estimate plume divergence and interactions with spacecraft surfaces [1]. A major limitation of these models is the accuracy of available near exit plane plume data for validation. The goal of this study is to characterize the near-plume velocity field of a 600 W Hall thruster using excited state ionic xenon laser-induced fluorescence (LIF). LIF is an ideal diagnostic for the investigation of plasma in the near-plume regions because it is a nonintrusive measurement. Unlike probe-based measurements, LIF will not perturb the local plasma or thruster operation.

This effort characterizes the external xenon ion velocity profiles of a midpower (600 W) Hall thruster at its nominal operating condition with a 300 V anode potential. Two orthogonal ion velocities are simultaneously probed using phase-sensitive detection in the near-field plume (less than 100 mm from the exit plane) in a three-dimensional volume. By the manipulation of the thruster location relative to the laser probe volume, we are able to measure axial, radial, and azimuthal ion velocities. Knowledge of these velocities provides insights into the extent of the external axial acceleration, the radial divergence of the ions in the plume, and the torque produced by the azimuthal motion of the exiting ions.

II. Xenon Ion Laser-Induced Fluorescence

LIF is a convenient diagnostic for the investigation of ionic and atomic velocities as it does not perturb the plasma as do other common diagnostic techniques, most notably electrostatic probes. For the results reported here, the $5d[4]_{7/2} - 6p[3]_{5/2}$ electronic transition of Xe II at 834.72 nm is probed. The isotopic and nuclear-spin effects contributing to the hyperfine structure of the $5d[4]_{7/2} - 6p[3]_{5/2}$ xenon ion transition produce a total of 19 isotopic and spin split components. The hyperfine splitting constants that characterize the variations in state energies are only known for a limited set of energy levels. Unfortunately, the 834.72 nm xenon ion transition only has confirmed data on the nuclear spin splitting constants of the $6p[3]_{5/2}$ upper state [2–5].

For velocity measurements, it is often convenient to probe optically accessible transitions for which there is incomplete knowledge of the isotopic and nuclear spin splitting constants. Hargus and Cappelli [2], Manzella [6], and Hargus and Charles [7] have previously used the $5d[4]_{7/2} - 6p[3]_{5/2}$ xenon ion transition at 834.72 nm to make velocity measurements in a Hall thruster plume. A convenient feature of this transition is the presence of a relatively strong line originating from the same upper state (the $6s[2]_{3/2} - 6p[3]_{5/2}$ transition at 541.9 nm) which allows for nonresonant fluorescence collection [8]. A nonresonant fluorescence scheme is preferred where there is the possibility of laser scattering from surfaces. The local velocity is determined by the spatially resolved measurement of the Doppler shift of the absorbing ions [9].

III. Experimental Apparatus

The LIF measurements were performed in a nonmagnetic stainless steel vacuum chamber with a 1.8 m diameter and 3 m length. It has a measured pumping speed of 32,000 L/s on xenon. Pumping is provided by four single-stage cryogenic panels (single-stage cold heads at 25 K) and one 50 cm two-stage cryogenic pump (12 K). Chamber pressure during thruster operation is approximately 6.7×10^{-3} Pa, corrected for xenon.

The Hall thruster used in this study is the circular 600 W Busek Company BHT-600 Hall thruster with a 3.2 mm hollow cathode. The acceleration channel of the thruster has a 32 mm outer radius and a 24 mm inner radius. The thruster has been characterized to have a thrust of 39 mN with a specific impulse of 1,530 s, yielding an efficiency of approximately 50%. A photograph of the circular BHT-600 Hall thruster is shown in Fig. 1. Table 1 shows the nominal operating conditions for the cylindrical BHT-600 thruster. During thruster operation, the parameters shown in Table 1 are monitored

Presented as Paper 5004 at the Joint Propulsion Conference, Hartford, CT, 21–23 July 2008; received 17 March 2009; revision received 26 June 2009; accepted for publication 6 July 2009.

*Senior Aerospace Engineer, Spacecraft Propulsion Branch. Associate Fellow AIAA.

†Scientist; currently U.S. Air Force Research Laboratory, Wright-Patterson Air Force Base, Ohio.

Fig. 1 Photograph of circular BHT-600 Hall thruster used in this study.

and recorded at a 1 Hz data rate by an automated data acquisition system.

The thruster is mounted on a three-axis orthogonal computer-controlled translation system. Figure 2 shows the Hall thruster within the vacuum chamber as well as the orientation of the two LIF probe beams. The laser is a tunable diode laser. It is capable of tuning approximately ± 50 GHz about a center wavelength of 834.72 nm. The 10 mW beam is passed through a Faraday isolator to eliminate feedback to the laser. The laser beam then passes through several beam pickoffs until it is focused by a lens and enters the vacuum chamber through a window. The probe beam is chopped at a frequency by an optical chopper (Ch2 at 2.8 kHz) for phase-sensitive detection of the fluorescence signal.

The two wedge beam pickoffs (BS) shown in Fig. 3 provide portions of the beam for diagnostic purposes. The first beam pickoff directs a beam to a photodiode detector (D1) used to provide constant power feedback to the laser. The second beam is divided into two equal components by a 50–50 cube beam splitter. The first component is directed to a commercial wavelength meter used to monitor absolute wavelength. The second component is sent through an optical chopper (Ch1 at 1.4 kHz) and through a low-pressure xenon hollow cathode discharge lamp. The lamp provides a stationary absorption reference for the determination of the Doppler shift. Unfortunately, there is no detectable population of the ionic xenon $5d[4]_{7/2}$ state. However, there is a nearby (estimated to be 18.1 GHz distant) neutral xenon $6s'[1/2]_1 - 6p'[3/2]_2$ transition at 834.68 nm [10,11]. The second pickoff sends a beam to a 300 MHz free spectral range Fabry–Perot (F-P) etalon that provides high resolution

Table 1 Nominal BHT-600 Hall thruster operating conditions

Anode flow	2.453 mg/s
Cathode flow	197 μg/s
Anode potential	300 V
Anode current	1.97 A
Keeper current	0.5 A
Heater current	3.0 A

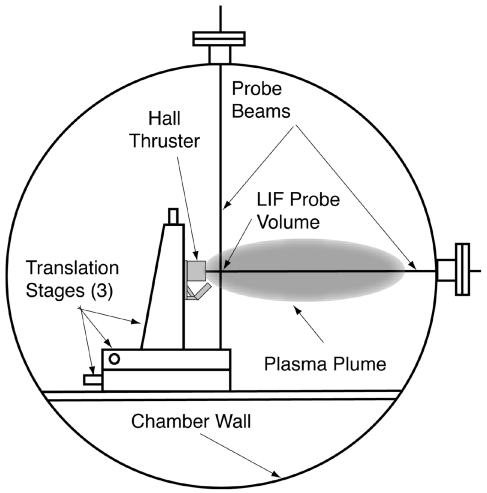

Fig. 2 Side view diagram of thruster within vacuum chamber showing the translation stages and two laser probe beams.

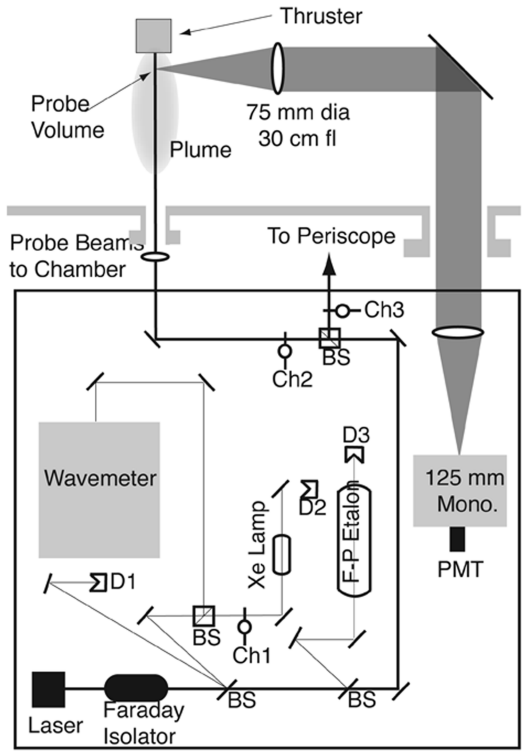

Fig. 3 Top view diagram of the laser optical train and collection optics.

frequency monitoring of the wavelength interval swept during a laser scan.

The fluorescence collection optics are also shown in Fig. 3. The fluorescence is collected by a 75-mm-diam, 300 mm focal length lens within the chamber. The collimated signal is directed through a window in the chamber side wall to a similar lens that focuses the collected fluorescence onto the entrance slit of 125 mm focal length monochrometer with a photomultiplier tube (PMT). The spatial resolution of the measurements is determined by the geometry of the entrance slit 1 mm width and 1.7 mm height (1:1 magnification collection optics).

The laser is controlled by an analog ramp signal generated by a multipurpose data acquisition system. During each laser scan, the data acquisition system records the absorption and two fluorescence signals generated by three dual-phase lock-in amplifiers. The signal from the Fabry–Perot etalon photodiode detector (D3) signal is also recorded after amplification and filtration using a current preamplifier. Typically, the scans span approximately 55 GHz. Each

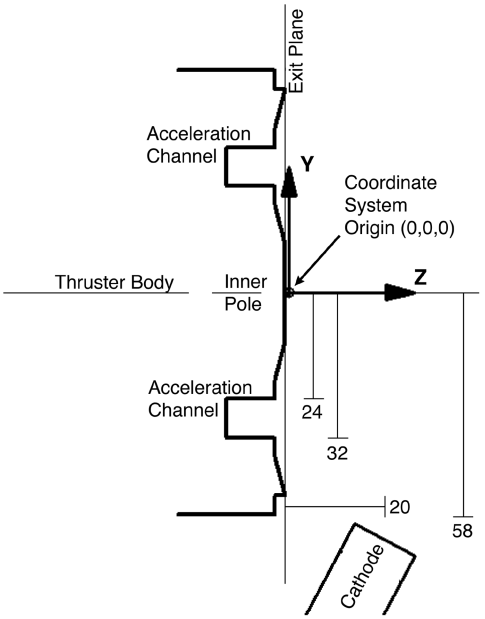

Fig. 4 Cross section of the Hall thruster geometry in the *Y*-*Z* axis with measurement reference origin and various dimensions (in millimeters) specified.

scan yields four data traces of several thousand points. The traces are then stored for postprocessing.

Figure 4 shows a cutaway view of the near-field geometry of the interrogated Hall thruster. The locations of the central magnetic poles and edges of the acceleration channel are indicated, as is the position of the cathode. The Cartesian coordinate system and origin used in these measurements are also shown in Fig. 4, with the positive X axis going into the page. The coordinate system orientation is also referenced in Figs. 2 and 3. The origin is at the center of the thruster face due to the ease and repeatability with which this position could be located. All measurements presented in this work will be located using these coordinates.

Although the majority of the measurements presented in this work are on the Y-Z plane ($X = 0$ mm), a significant number of data were also taken on the X-Z plane ($Y = 0$ mm). In the Y-Z plane, the vertical probe beam shown in Fig. 2 will sample the radial ion velocities. In the X-Z plane, the same probe beam will sample the azimuthal ion velocities. We are only aware of two other azimuthal ion velocity measurements in the literature [6,12]. The most complete, performed by Manzella [6], used a retroreflection technique.

IV. Experimental Results

In this work, we have chosen to represent the bulk ion velocities by using the shift of the peak of the fluorescence trace. In most cases, this provides an unambiguous indication of the bulk velocity of the ion stream at a location determined by the translation stage in a volume dictated by the collection optics and laser beam waist (1–1.7 mm length by 200 μm diameter). This corresponds to the peak of the velocity distribution, which is near the mean for many cases.

Because of several factors, the absolute uncertainty of the reported velocities is estimated to be ± 500 m/s. The first and most important factor is the uncertainty in the relative neutral and ionic transition energies. The second source of uncertainty is the broadening of the line shape, which is indicative of a broadened velocity distribution. Therefore, there is some ambiguity as to the location of the shifted peak. This distribution is often not consistent with a Maxwellian distribution, and, as such, does not necessarily indicate a temperature. There is also some evidence that the broadening of the traces, in part, is due to the 20–40 kHz breathing mode oscillation typical of Hall thrusters [13].

We recognize the portions of the plume where distinct ion velocity populations interact by the appearance of more than one recognizable velocity population. In these cases, the distinct peaks are each assigned a velocity. In all cases, the peaks are within the quoted uncertainty of ± 500 m/s or better. In fact, the repeatability (precision) by which the peaks are located appears to be a fraction of the quoted uncertainty ($\approx \pm 100$ m/s). However, the fluorescence line shapes are often significantly broadened in these areas of the plume where there is interaction between several velocity distributions. This broadening is presumably due to wide velocity distributions produced by the mechanism governing the flow interaction. It is not clear from this work which flow interaction mechanism gives rise to a Hall thruster plume's distinct central luminous core. In light of the complexity of the plume flow structure, the quoted uncertainty in the value of the velocities should be viewed as the uncertainty in the determination of the peak of the fluorescence line shape. In most of the plume, this will correspond to the mean velocity of the ion population. When multiple velocities are given for a single location (and there are usually ions with intermediate velocities), the vast majority of the ions are well characterized. However, the relative weighting is not readily apparent. Furthermore, there is a degree of arbitrariness in the assignment of minimum peak levels to determine what constitutes a significant velocity population. It is possible to extract velocity distributions from the raw fluorescence traces; however, these techniques typically require higher signal-to-noise ratios than available in this study [14].

A. *Y*-*Z* Plane Ion Velocity Field

As previously stated, a large number of ion velocity measurements were taken in the Y-Z plane ($X = 0$ mm). These take advantage of the nearly symmetrical flow of xenon ions exiting the Hall thruster. In the Y-Z plane, the Y velocity component uniquely corresponds to the radial velocity of the ions exiting the Hall thruster. As always, the Z velocity component is the Hall thruster axial ion velocity.

Figure 5 shows the Y-Z velocity field measured in this study for the nominal operating conditions. As shown, the ions diverge as they emerge from the thruster acceleration channel. The ions are externally accelerated axially as well as radially. This results in considerable divergence from the exit of the acceleration channel annulus. As a result, there is divergence of the plume both inward and outward of the plume centerline with ions flowing at highly oblique angles to the plume (Z) axis. This divergence is coupled with significant ion focusing toward the plume centerline. This produces regions where more than one distinct ion velocity is present in Fig. 5. The most prominent region where this occurs is the central core of the plume. Beginning at approximately 50 mm downstream of the exit plane in the flow center, the radial velocities exhibit two peaks and are correspondingly assigned two velocity vectors. It is believed that this region is an area of flow mixing, as ions from different sides of the acceleration annulus interact. The precise form of the interaction is not completely clear and several mechanisms can be considered ranging from ion collisional excitation to a low-density electrostatic shock [15]. These relatively low radial velocity ions correspond to the bright central core exhibited in Hall-type thrusters. Nearly identical behavior has been observed in prior measurements and to a

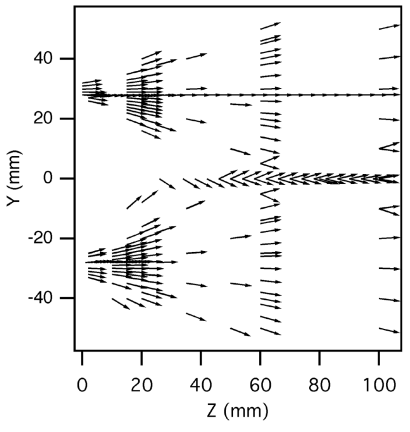

Fig. 5 Ion velocity vector plot in the *Y*-*Z* plane ($X = 0$).

greater extent with a similar 200 W Hall effect thruster, primarily due to its smaller physical size, which allows interrogation of a larger number of thruster diameters downstream [7]. In this previous study, there was also a region with two distinct axial velocity populations. It was detected 2 diameters downstream and appeared to correspond to the edges of the visible plume. This effect is not as clearly discernible for this medium power Hall thruster due to the study volume only extending 1.6 exit diameters into the plume. Otherwise, the plume is remarkably similar to this previous study.

Figure 6 presents the velocity component profiles measured in the Y-Z plane that were used to create the vector plot in Fig. 5. At the thruster exit ($Z = 0$ mm), the axial velocity is approximately 17 km/s (197 eV), but the radial velocity profile across the acceleration channel is sharply sloped, varying from $+5$ to -5 km/s, indicative of the degree of initial plume divergence. On the thruster face centerline, there is a very different ion population. This region appears to consist of very low-velocity ions, possibly in some sort of isolated recirculation zone, or products of charge exchange collisions with background atoms. Signal strength at the exit plane was affected by the thruster current oscillations. The effect appeared to lessen with measurements further downstream. The thruster current oscillations appear to have affected the signal-to-noise ratio of the LIF traces at $Z = 0$ mm, and there appears to be additional uncertainty in several of these measurements.

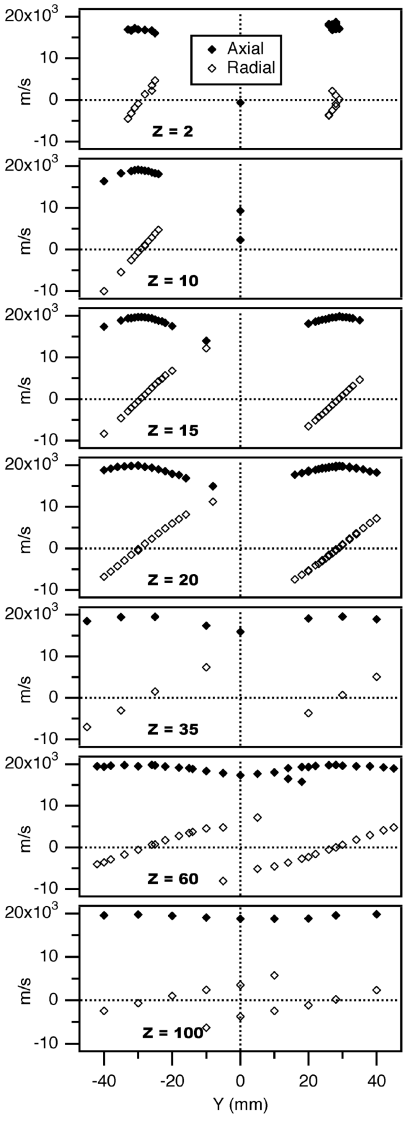

Fig. 6 Ion velocity components for various locations in Z on the Y-Z plane. The closed symbols represent axial (Z) velocity components and the open symbols represent the radial (Y) velocity components.

Further downstream into the plume, the axial velocities develop as they simultaneously diverge, due to the steep radial velocity gradient, and undergo external axial acceleration. Ultimately, the external acceleration increases the terminal axial velocity to 19.8 km/s (267 eV), indicating that approximately 70 eV of additional energy is deposited into the ion population in the near-plume region. As the plume evolves, the curvature of the axial velocity profiles flattens. At $Z = 35$ mm, the flows from the opposite sides of the annulus appear to meet and begin to interact. Beyond this axial location, there is considerable evidence of interaction between the ion populations within the flow, as multiple radial, and occasionally axial, velocities are common. This is most clearly illustrated at $Z = 100$ mm where the interaction between the various ion populations is most readily evident by the overlap of radial velocity profiles.

Figure 7 shows the axial velocity evolution in the $Y = +28$ mm, $X = 0$ mm line located at the center of the acceleration channel annulus and extending axially into the plume. The external acceleration is completed by $Z = 20$ mm, which corresponds to the Z position of the cathode. However, it can be assumed that plasma equipotential lines do not follow the physical placement of the cathode. As stated earlier, the external acceleration is approximately 70 eV and represents 26% of the ion kinetic energy, a sizable fraction of the 267 eV maximum axial ion energy.

Similar to Fig. 7, Fig. 8 shows the axial (Z) and radial (Y) velocity components taken along the $X = Y = 0$ line. This is an interesting region for study because it interrogates the apparent recircularization and/or backflow zone near the thruster face at the origin of the coordinate system used in this paper. This region is interesting in that long duration firings of similar thrusters have developed regions of surface erosion, presumably due to sputtering. A very similar rectangular 600 W thruster experienced considerable erosion on the thruster face following an extended operation, particularly on the surface of the central magnetic core. Figure 9 illustrates photographically the extent of the erosion on the central core, where ion sputtering has removed the alumina coating that protects the face of the thruster from the ambient plasma.

B. Three-Dimensional Ion Velocity Field

Figure 10 shows Z and Y velocity components measured at four different positions about the thruster. These correspond to the

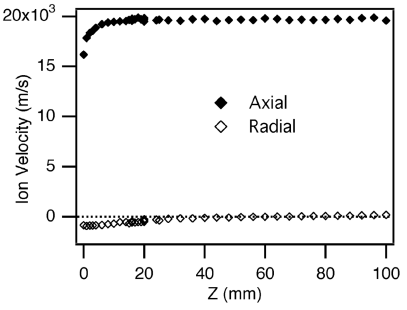

Fig. 7 Acceleration channel center axial (Z) and radial (Y) velocity components at $Y = 28$ mm, $X = 0$.

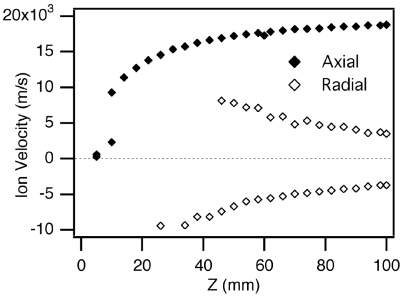

Fig. 8 Acceleration channel center axial (Z) and radial (Y) velocity components at $X = Y = 0$ mm.

Fig. 9 Front surface erosion of a rectangular BHT-600 thruster following extended operation. Note the exposed metal at the thruster center where the protective alumina covering has been eroded.

acceleration channel centerline location at the thruster's four cardinal directions. This plot shows some of the expected symmetry, particularly for the Y velocity component, which, in this case, can either be the Hall thruster radial velocity or the azimuthal velocity. Ideally, the Z velocity profiles would be identical; however, this does not appear to be the case. As shown in Fig. 4, the cathode is located on the negative Y axis and closest to the $Y = -28$ mm, $X = 0$ mm cardinal. Interestingly, the velocity data on this cardinal exhibit a marked departure from the other data sets, which are all very similar and exhibit higher thruster exit velocities than does this data set nearest the cathode. We are not aware of any previous studies which have directly demonstrated this degree of nonuniform axial acceleration due to the cathode; however, we are aware of one published numerical study showing that proximity to the cathode may produce an azimuthal dependency on the axial plasma potential profiles [16]. Although at least one previous study has postulated azimuthal variations in the axial plasma potential profiles producing measurable nonuniform erosion in a Hall-effect-type thruster, the effect was linked to similar nonuniformities in the magnetic field once propellent flow nonuniformities were eliminated as the cause [17]. In addition, the plume of neutrals exiting the cathode may locally enhance classical electron mobility and thereby affect the ion acceleration.

The possibility of thruster misalignment has been largely eliminated as a possible source of the differing axial acceleration profiles shown in Fig. 10. Before the measurements, the Y-axis motion was confirmed to be parallel to the thruster front face to within

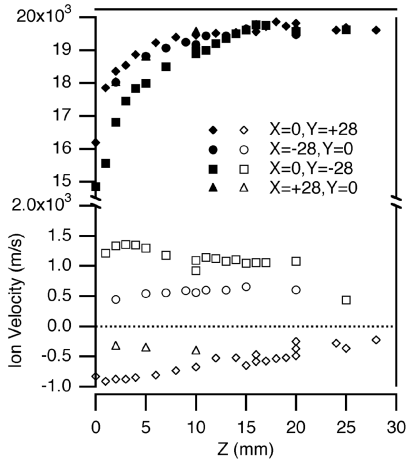

Fig. 10 Z-axis and Y-axis ion velocity profiles for channel center ($R = 28$ mm, where $X^2 + Y^2 = R^2$) at the four coordinate cardinal directions. Note the solid symbols denote the Z velocity component and the open symbols the Y velocity component.

1 mm across the ± 54 mm of the thruster front face. The same procedure was followed with similar results for the X axis. This alignment was confirmed following the acquisition of the data presented in this work. These measurements do not completely exclude the possibility of minor thruster manufacturing misalignments, but these appear unlikely to produce the results seen. It is, however, obvious that these data raise several questions that require further study.

Depending on location of the LIF interrogated volume, it is possible to measure the azimuthal velocity of the ions. This may be performed by examining the Y-axis velocity component on the X-Z plane with $Y = 0$. The electron Hall current is azimuthal within the acceleration channel of the thruster and is responsible for the closed electron drift on which Hall effect thrusters rely to function. A major premise of the operation of these electrostatic thrusters is that the electrons are magnetized and the ions are not, primarily due to the 2.4×10^5 ratio in the relative masses despite the 100 times higher electron temperature. This results in Larmor radii for the electrons on the order of millimeters, whereas the ion Larmor radii are estimated to be on the order of several tens of centimeters. However, it is known that ions do possess some azimuthal component to their velocities and this has not been extensively studied.

Figure 11 shows both a plot of the Z velocity component and the measured azimuthal velocity component at $X = \pm 27$, ± 28, and ± 29 mm, $Y = 0$, and $Z = 5$ mm. The azimuthal component can be estimated to be the mean (475 m/s) of the Y velocity components from $X = \pm 28$ mm. Assuming that the Hall thruster ionizes 100% of the xenon propellant and using the mean radius as a reference, the torque produced by the thruster is estimated to be 3.2×10^{-5} Nm. The 475 m/s azimuthal velocity for this 600 W thruster is larger than the 250 m/s measured on a 1.35 kW SPT-100 Hall thruster by Manzella [6]. However, this is consistent with scaling relations that would lower the magnetic field as the thruster geometry grows. Using the ratio of the outer diameters (64 mm for the BHT-600; 100 mm for the SPT-100), the measured ion azimuthal velocities are very nearly inversely proportional to acceleration channel diameter. This is also in proportion to the magnetic field, as predicted from Hall thruster geometrical scaling arguments for constant accelerating potential [18].

Less well understood is the azimuthal velocity axial evolution in the plume. Figure 12 examines the azimuthal velocity into the plume from the exit plane to 100 mm distant. The azimuthal velocity appears to grow some in the near plume. This is not surprising because a significant fraction of axial ion acceleration occurs outside

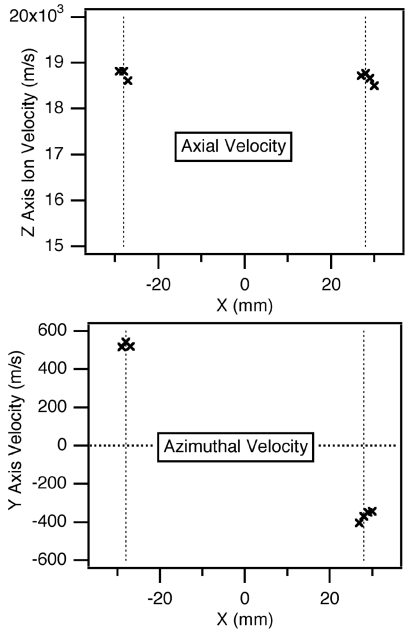

Fig. 11 Axial and azimuthal velocities at $X = \pm 27, \ldots, \pm 30$ mm, $Y = 0, Z = 5$ mm.

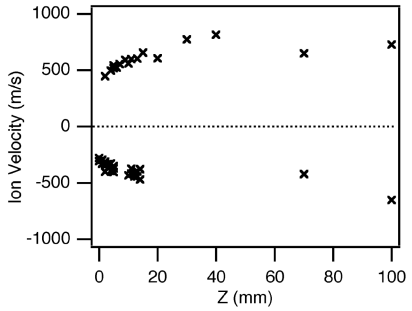

Fig. 12 Azimuthal velocity evolution in to the plume ($X = \pm 27, \ldots, \pm 30$ mm, $Y = 0$, $Z = 0$–100 mm).

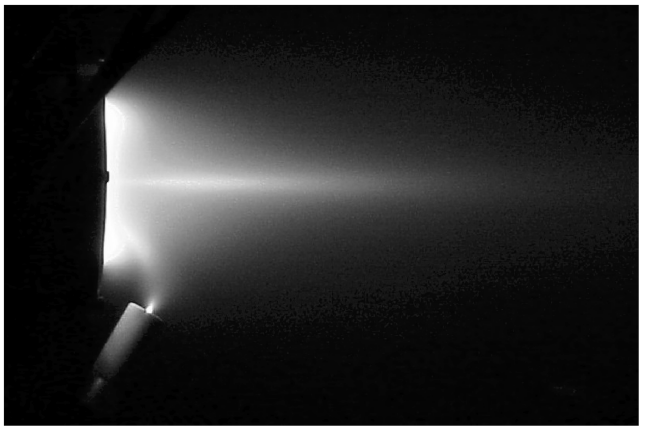

Fig. 13 Photograph of the cylindrical BHT-600 Hall thruster plume with the plume central core clearly identifiable.

the physical confines of the acceleration channel. It is therefore logical to assume that some portion of the electron Hall drift current also is flowing outside the thruster. This may explain the apparent increase in the azimuthal velocity in the same 20 mm near exit plane region where Figs. 7 and 10 show all the external acceleration to have been completed. It is interesting to note that the azimuthal velocity is clearly discernible throughout the measurement volume and likely further downstream.

V. Conclusions

The ion flowfield in the near-plume region of a xenon 600 W Hall effect thruster is characterized using LIF for a single nominal operating condition with an anode potential of 300 V. The flow is reasonably complex in that there are interactions between various ion populations which are not fully understood, but may be collisional or related to electrostatic shocks which may produce the luminous central core of the plume, as illustrated in Fig. 13. The physical extent of the central core feature correlates closely to where multiple radial velocity components are shown in Fig. 5. This bright jet feature is presumably caused by a yet to be definitively identified interaction between the multiple ion population streams and possibly background neutrals in the vacuum test facility.

Significant external ion acceleration occurs and is consistent with that seen in other Hall thrusters. Approximately 70 eV of energy is added to the axial energy of the ions. Uniquely, this series of measurements examined the uniformity of the axial ion acceleration and found differences that were particularly significant nearest the cathode neutralizer. At this location, the exit plane velocity was lowest, although the external acceleration did produce a uniform axial velocity 20 mm downstream of the thruster exit.

This study also measured the 475 m/s azimuthal velocity on two sides of the Hall thruster. These measurements yielded azimuthal velocities inversely proportional to the thruster characteristic geometry (in this case, the outer diameter of the acceleration channel) when compared to previous LIF measurements of the SPT-100 by Manzella [6]. Invoking geometrical Hall thruster scaling, this shows the azimuthal ion velocity component to be approximately proportional to the applied magnetic field. It is interesting to note that azimuthal velocity increases in the same region where the external axial acceleration occurs, which is consistent with the supposition that a portion of the electron Hall drift current is closed in the near-field plume.

This effort has only examined the near exit plane velocity field of a single operating condition. To fully characterize this thruster, several other operating conditions also require careful examination. One item of future interest is understanding the effect of the vacuum chamber conditions, particularly background pressure, on the plume dynamics of Hall thrusters. This would be best served by extending velocity measurements into the acceleration channel to fully characterize the ion acceleration [13,19].

Another important issue is that the concept of a single velocity, or even several distinct velocities, is inadequate, particularly in regions where significant interactions of velocity populations occur. Although the concept of a single ion velocity remains useful for the presentation and interpretation of LIF data, it is also possible to view the resulting fluorescence line shapes as an indication of the velocity distribution [14]. A more accurate analysis of the true plume ion dynamics would be to extract velocity distribution functions from fluorescence traces. This would provide valuable data for comparison with various existing Hall thruster device models and simulations.

Acknowledgments

The authors would like to thank the contributions of C. Niemela, M. Nakles, and G. Reed for their assistance in the analysis of the laser-induced fluorescence data. We would also like to thank C. Larson for a series of very insightful comments and suggestions regarding Hall thruster life processes and near-plume plasma dynamics.

References

[1] Nakles, M. R., Brieda, L., Reed, G. D., Hargus, W. A. Jr., and Spicer, R. L., "Experimental and Numerical Examination of a Hall Thruster Plume," Electric Rocket Propulsion Society Paper No. 2007-073, 2007.

[2] Hargus, W. A., Jr., and Cappelli, M. A., "Laser-Induced Fluorescence Measurements of Velocity Within a Hall Discharge," *Applied Physics B: Lasers and Optics*, Vol. 72, No. 8, June 2001, pp. 961–969. doi:10.1007/s003400100589

[3] Geisen, H., Krumpelmann, T., Neuschafer, D., and Ottinger, C., "Hyperfine Splitting Measurements on the 6265 Angstrom and 6507 Angstrom Lines of Seven Xe Isotopes by LIF on a Beam of Metastable Xe (3P0,3) Atoms," *Physics Letters A*, Vol. 130, Nos. 4–5, July 1988, pp. 299–309. doi:10.1016/0375-9601(88)90614-7

[4] Fischer, W., Huhnermann, H., Kromer, G., and Schafer, H. J., "Isotope Shifts in the Atomic Spectrum of Xenon and Nuclear Deformation Effects," *Zeitschrift für Physik*, Vol. 270, No. 2, Jan. 1974, pp. 113–120. doi:10.1007/BF01677442

[5] Bronstrom, L., Kastberg, A., Lidberg, J., and Mannervik, S., "Hyperfine-Structure Measurements in Xe II," *Physical Review A*, Vol. 53, No. 1, Jan. 1996, pp. 109–112. doi:10.1103/PhysRevA.53.109

[6] Manzella, D. H., "Stationary Plasma Thruster Ion Velocity Distribution," AIAA Paper No. 1994-3141, June 1994.

[7] Hargus, W. A., Jr., and Charles, C. S., "Near Exit Plane Velocity Field of a 200 W Hall Thruster," *Journal of Propulsion and Power*, Vol. 24, No. 1, Jan.–Feb. 2008, pp. 127–133. doi:10.2514/1.29949

[8] Hansen, J. E., and Persson, W., "Revised Analysis of Singly Ionized Xenon, Xe II," *Physica Scripta*, Vol. 36, No. 4, 1987, pp. 602–643. doi:10.1088/0031-8949/36/4/005

[9] Demtroder, W., *Laser Spectroscopy: Basic Concepts and Instrumentation*, Springer–Verlag, Berlin, 1996.

[10] Miller, M. H., and Roig, R. A., "Transition Probabilities of Xe I and Xe II," *Physical Review A*, Vol. 8, No. 1, July 1973, pp. 480–486. doi:10.1103/PhysRevA.8.480

[11] Moore, C. E., *Atomic Energy Levels*, Vol. 2, National Bureau of Standards, Washington, D.C., 1958.

[12] Williams, G. J., Smith, T. B., Gulczinski, F. S., Beal, B. E., Gallimore, A. D., and Drake, R. P., "Laser Induced Fluorescence Measurement of Ion Velocities in the Plume of a Hall Effect Thruster," AIAA Paper No. 1999-2424, June 1999.

[13] Hargus, W. A., Jr., Nakles, M. R., Pote, B., and Tedrake, R., "The Effect of Thruster Oscillations on Axial Velocity Distributions," *Proceedings of the 44th Joint Propulsion Conference and Exhibit*, American Institute of Aeronautics and Astronautics Paper No. AIAA-2008-5004, Hartford, CT, July 2008.

[14] Hargus, W. A. Jr., and Nakles, M. R., "Evolution of the Ion Velocity Distribution in the Near Field of the BHT-200-X3 Hall Thruster," AIAA Paper No. 2006-4991, July 2006.

[15] Hruby, V., Monheiser, J., Pote, B., Rostler, P., Kolencik, J., and Freeman, C., "Development of Low Power Hall Thrusters," AIAA Paper No. 1999-3534, June 1999.

[16] Parra-Diaz, F. I., "Development of a Model for the Near-Exit Plume of a Hall Thruster," M.S. Thesis, Massachusetts Inst. of Technology, Cambridge, MA, Jan. 2007.

[17] Marrese, C., Polk, J., King, L., Garner, C., Gallimore, A. D., Semekin, S., Tverdoklebov, S., and Garkusha, V., "Analysis of Anode Layer Thruster Guard Ring Erosion," Electric Rocket Propulsion Society Paper No. 1995-196, 1995.

[18] Khayms, V., and Martinez-Sanchez, M., "Stationary Plasma Thruster Ion Velocity Distribution," AIAA Paper No. 1996-3291, July 1996.

[19] Nakles, M. R., and Hargus, W. A., Jr., "The Effect of Background Pressure on the Acceleration Profile Within a Medium Power Hall Thruster," AIAA Paper No. 2008-5101, July 2008.

J. Blandino
Associate Editor